

Tuning Magnesium-Air Fuel Cell Performance and Corrosion Behavior through Electrode and Electrolyte Configuration

Nurul Shahzira Hazri^a, Sahriah Basri^{a,*}, Azran Mohd Zainoodin^a, Mismisuraya Meor Ahmad^b & Siti Kartom Kamarudin^{a,c}

^a*Fuel Cell Institute, Universiti Kebangsaan Malaysia, 43600 Bangi Selangor, Malaysia.*

^b*Faculty of Chemical Engineering & Technology, Universiti Malaysia Perlis (UniMAP), 02600 Arau, Perlis, Malaysia*

^c*Faculty of Engineering and Built Environment, Universiti Kebangsaan Malaysia, 43600 UKM Bangi, Selangor, Malaysia*

*Corresponding author: sahriah@ukm.edu.my

Received 20 August 2024, Received in revised form 21 October 2024
 Accepted 21 November 2024, Available online 30 January 2025

ABSTRACT

Magnesium-air fuel cell (MAFC) is a hybrid system that combines the design of a fuel cell and a battery, requiring a constant replacement of anode and electrolyte to operate. MAFC application is limited for short-term high-power applications like emergency and portable power supplies because of severe corrosion problems impairing the performance of MAFC. Hence, this study focuses on performance by investigating the effect of electrolyte volume, electrodes position, and electrolyte concentration on performance of Mg-air fuel cell. Three sets of experiments were conducted starting with variation in volume of electrolyte. Then, it is applied in the cell configuration to test the MAFC performance with different electrode position. Lastly, the best electrode position is applied to the new modified MAFC together with the chosen electrolyte to investigate the effect of electrolyte concentration on MAFC performance. Finding shows that electrolyte volume not really significant to the performance while higher NaCl concentration can increase the performance of MAFC significantly. 10 wt% of NaCl produce the highest power density of 38.95 mW.cm⁻² and operating voltage of 1.67 V. Unfortunately, higher corrosion rate was observed in higher NaCl concentration. Finally, adding sodium phosphate act as corrosion inhibitor manage to suppress the corrosion reaction and lowers the corrosion rate.

Keywords: Cell configuration; corrosion; magnesium; magnesium-air fuel cell; metal-fuel cell

INTRODUCTION

The accelerating energy transition movement from fossil fuel to renewable and green energy has boosted the growth of the technology of renewable energy sources to meet global electricity demand while supporting the 7th sustainable development goal of providing affordable, reliable, sustainable and modern energy for all (Gielen et al. 2019). Besides the well-known renewable alternative such as solar and wind energy, which has made excellent progress in the last decade, electrochemical energy storage and device such as the metal-air fuel cell has become a clean energy alternative and remains under progressive development. Metal-air fuel cell has gain attention from researchers because of their impressive energy density and

huge potential to replace lithium-ion battery, particularly in the automotive industry, and it is environmentally friendly, because it produce zero carbon emission and non-toxic discharge product (Liu et al. 2020). Metal-air fuel cell or battery is a hybrid fuel cell that possesses both a battery and fuel cell feature. Generally, metal-air fuel cell is composed of three components, namely, metal anode, alkaline or acidic electrolyte and air cathode. Many common metals have been developed and are still developing for metal-air fuel cell as anode, including Li, Na, K, Zn and Mg (Häcker et al. 2023; Samarasingha et al. 2021; Tong et al. 2021).

Among all the metal anode in metal-air fuel cell, Mg-air fuel cell that utilizes magnesium as anode has the second highest theoretical energy density (2,843 Wh Kg⁻¹)

next to Li–air (3,463 Wh Kg⁻¹) and highest theoretical voltage (3.1 V). Mg–air fuel cell also benefits from the abundance of Mg source in the Earth crust, indirectly making it economic and affordable for commercialisation (Tong et al. 2021; Zhang et al. 2014). Mg–air has a simple working principle; it is only activated in the presence of electrolyte. Once electrolyte is added into the cell, Mg is oxidised to produce Mg ion and electrons. Simultaneously, electrons are transmitted from the anode to the cathode *via* an external circuit, resulting in the generation of electricity. Meanwhile, the catalyst at the cathode site catalyses oxygen reduction reaction (ORR), causing the oxygen, water, and electrons to react, forming hydroxide ions. The overall reaction occurring in the electrolyte produces magnesium hydroxide (Mg (OH)₂) precipitate and hydrogen gas. Considering that Mg–air fuel cell is easy to assemble and operate, and Mg is lightweight with a density of 1.74 g cm⁻³, it is easy to carry around, and the existing commercial Mg–air fuel cells are used as emergency back-up power in schools and hospitals and portable power for outdoor activities. Moreover, Mg–air fuel cell is used for military and underwater application because it utilises seawater or saltwater as electrolyte (Chen et al. 2020; DENG et al. 2016).

Magnesium-air fuel cell suffers from severe corrosion due to the imbalance of reaction speed at Mg anode and air cathode, where the Mg anode reacts vigorously as soon as it comes to contact with the electrolyte and the sluggish ORR reaction at the cathode leads to precipitation production, thus deteriorating Mg–air and is unstable for long-term application (Saji 2023; Song 2013a, 2013b). Magnesium is thermodynamically active but unstable, meaning that it will oxidise quickly in any environment that contains water or oxygen. This makes magnesium prone to corrosion. The reason for this is because magnesium has a very low standard electrode potential value (-2.37 V vs. SHE), which makes it very easy for it to donate electrons and form ions, which initiates the oxidation process (Deng et al. 2019). Besides the nature of the reaction, galvanic corrosion is also induced by the presence of various impurities such as iron, nickel or copper in the alloy and inhomogeneous microstructure due to the fabrication process of magnesium alloy that leads to the formation of micro cathodes in the alloy (Alloys & 2021 n.d.; Amjad Javaid & Frank Czerwinski 2021; Tong et al. 2021).

Accordingly, many studies have focused on altering the microstructure of magnesium anode such as using magnesium alloy (Guo et al. 2022; Song & Atrens 2003), trying different fabrication techniques (Amjad Javaid & Frank Czerwinski 2021), and applying coating (Ashassi-Sorkhabi et al. 2019; Zai et al. 2020) to improve the corrosion resistance of magnesium alloy. For example,

Chen et al. assessed how alloying with La and Ce affected a modified Mg-2Zn magnesium alloy's discharge performance (Chen et al. 2022). The findings showed that alloying elements were able to lower the rate of self-corrosion and inhibit the anodic hydrogen reaction by introducing second-phase Mg-Zn-La-Ce particles into the magnesium matrix. At 40 mA cm⁻², the Mg-2Zn-La-Ce anode can generate 1,311 mAh g⁻¹ of specific energy with 60% anodic efficiency. For its counterpart, the air cathode, manganese has recently become attractive in developing a more efficient electrocatalyst for Mg–air fuel cell to improve the oxygen reduction reaction (Dong et al. 2022; Zhao et al. 2022b, 2022a). Zhou et al. adopt hydrothermal method to synthesis copper-doped-MnO₂ (Cu–MnO₂) nanowires with varying amounts of Cu²⁺ (Zhou et al. 2022). The electrocatalytic results indicate that Cu–MnO₂ exhibits superior ORR activity than pristine α -MnO₂ due to lower charge transfer resistance and increased kinetic rate. Mg-air battery with Cu-MnO₂ electrocatalyst yield a peak power density of 73.4 mW cm⁻² and a high discharge voltage. Moreover, the addition of corrosion inhibitor in electrolyte has been explored extensively including green inhibitor to improve the corrosion and precipitation issue in the work of Lamaka et al. (Lamaka et al. 2017).

To date, studies on the physical design factors of cells or the configuration of magnesium-air fuel cells is an underrated topic creating a gap in the development of magnesium-air fuel cell. For example, Xue et al. [26] first studied the gas diffusion layer (GDL) in magnesium-air fuel cells (Xue et al. 2015). The catalyst layer, current collector layer, and gas diffusion layer are the components of the cathode structure. The oxygen reduction process takes place at the three-phase boundary (TBP) between air, liquid electrolyte, and solid catalyst electrode. The gas diffusion layer permits continuous and limitless oxygen from the surrounding air to pass through this TBP. Thus, a high electronic conductivity to transmit electrons, a waterproof structure to prevent leaks, and a high oxygen diffusion rate to lessen polarisation are the characteristics of an ideal gas diffusion layer. One of GDL's drawbacks is that airborne particles can quickly obstruct the pore channels, which lowers the material's gas diffusion coefficient over time. Thus, Xue et al. used a straightforward silica template technique to create super-hydrophobic GDLs with linked regular pores, and then evaluated their electrochemical characteristics in a magnesium-air fuel cell (Xue et al. 2015). The findings indicate that a high gas permeability coefficient of GDL can be achieved by employing a 30% silica template, which results in an interconnected and homogenous pore structure. Magnesium-air cells with 30% normal pore size have a maximum power density of 88.9 mW cm⁻², which is around 1.2 times that of pure GDL. Large magnesium

anode current collector design optimisation has drawn attention recently for large-scale magnesium-air primary battery applications. Kim et al. looked at how various current-collector contact points (CCP) affected the performance of electrochemical discharge and the anode degradation of magnesium (Kim et al. 2022). The findings indicate that choosing the right CCP for the magnesium anode is crucial for boosting discharge capacity. The position of the CCP on the magnesium anode determines the considerable variations in the current levels recorded at various anode surface regions. It is believed that the primary reason for the unintended breakdown of magnesium anodes after discharge is this uneven current distribution. Multiple ideal CCPs have been constructed to minimise the degradation of the magnesium anode during the discharge process by minimising the local concentrated current around the magnesium anode CCP through numerical simulations based on electric field analysis. When compared to magnesium anodes with a single CCP (38.7%), magnesium anodes with several CCPs demonstrated superior energy conversion efficiency (42%) and discharge capacity (46.2 Ah).

Based on literature review, design factor concerning electrolyte volume or positioning of electrode for MAFC has yet been researched while it is a common topic in Li-ion battery system and other fuel cell such as microbial fuel cell. For instance, An et al. had investigated the relationship between electrochemical performance and the electrolyte volume of Li-ion pouch-cells consisting of 1.2 M LiPF_6 and graphite/ $\text{Li}_{1.02}\text{Ni}_{0.50}\text{Mn}_{0.29}\text{Co}_{0.19}\text{O}_2$ (NMC-532) electrodes in ethylene carbonate:ethylmethyl carbonate (EC:EMC) electrolyte (An et al. 2017b). It is shown that an electrolyte volume factor of 1.9 times the total pore volume of cell components (cathode, anode, and separator) is necessary for low impedance and long-term cyclability. Additionally, after 100 cycles, the resistance ratios for the charge transfer and passivation layers at the cathode were 1.5–2.0 higher than the original values, demonstrating that lower electrolyte levels lead to higher observed ohmic resistances. Compared to the passivation layers, the cathode had a resistance to charge transfer that was two to three times higher. Recently, Simeon and Freitag investigated the behaviour of a soil microbial fuel cell in a fed batch setting using synthetic urine medium (SUM) at electrode spacings of 2, 5, and 8 cm (Simeon & Freitag 2022). Results revealed that the cell with 8 cm electrode spacing produce highest power density which is 271.1 mW cm^{-2} . It is observed that initially better performance was yield with the smaller electrode spacing because of lower internal resistance. However, larger electrode spacing is more beneficial to yield maximum performance though it requires more time to achieve stability. Another work by Thir et al. investigated the effect of electrode distance on

the efficiency of photocatalytic fuel cell integrated electro-Fenton (PFC-EF) system as it influence the mass transfer of ions in the system (Thor et al. 2022). They found that shorter distance between electrode is desirable for generation of electricity where in the study, PFC-EF system with 2 cm electrode spacing yield the highest power output of $25.39 \mu\text{W}$. They explained that the closer distance is responsible in reducing the resistance of ion flow and further enhanced the ion transfer between electrodes. In view of this, the design factor such as the electrodes position or spacing and electrolyte volume are important aspects that should be considered to obtain a rational design for magnesium-air fuel cell. Herein, the effect of electrolyte volume and electrode position in different electrolyte concentration on the performance of Mg-air fuel has been investigated to find out the optimum cell configuration to yield maximum performance.

EXPERIMENTAL

Three factors in cell configuration of a MAFC are determined in this work to find the optimum configuration to obtain highest performance of MAFC. The factors involved are volume of electrolyte, position of electrodes, and electrolyte concentration. Three sets of experiments were conducted starting with variation in volume of electrolyte. After determining the optimum electrolyte volume, it is applied in the cell configuration to test the MAFC performance with different electrode position. Lastly, the best electrode position is applied to the new modified MAFC together with the chosen electrolyte to investigate the effect of electrolyte concentration on MAFC performance. Figure 1 below summarized the flow of experiment for optimum cell design.

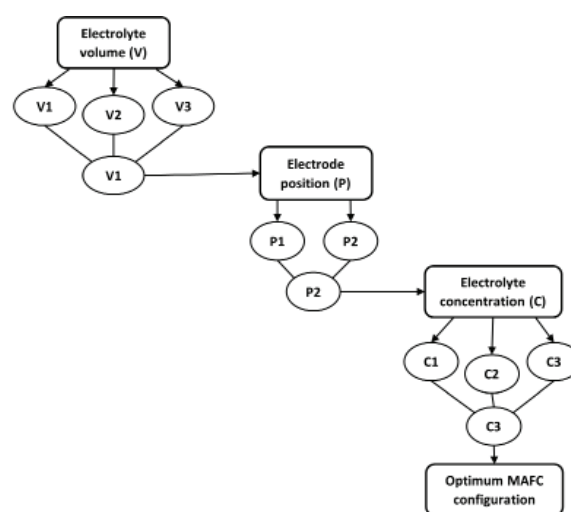


FIGURE 1. Methodology flow chart

SAMPLE PREPARATION

Mg–3Al–1Zn (AZ31) was used in this work where the chemical composition is mainly made up of 3 wt.% aluminium, 1 wt.% zinc, and the remaining is magnesium. AZ31 is a commercial magnesium alloy and well-known for its low mass density, good mechanical properties and good corrosion resistance hence have been used in many industries such as aircraft and automotive (Luo et al. 2020; Zai et al. 2020; Zhang et al. 2022). The alloy used was as cast and cut into 100 mm × 100 mm × 1 mm plate. The surface was polished with silicon carbide sandpaper up to 1,200 grit to remove the oxidation layer, rinsed with alcohol and then dried in cold air. Commercial table salt and deionised water were used to prepare the 3.5 wt.% salt solution as the electrolyte. The purpose of utilizing commercial table salt instead of analytical grade chemical NaCl is because this work would like to demonstrate the

commercial application of emergency domestic power supply as table salt is far cheaper and easier to obtain.

MAFC PERFORMANCE TEST

A modified Wattery Single Cell battery as shown in Figure 2 has modified to include sediment space inside the chamber. A readymade air electrode with MnO₂ catalyst as the cathode were used to examine the performance of MAFC. MEET Co. Ltd. also supplied the anode, which was AZ31. NaCl 3.5 wt.% was used as electrolyte as it is the commonly used concentration for MAFC. The reaction regions for both anode and cathode were 70 cm². The curves of cell voltage and power density versus current density were obtained. Figure 3 shows the schematic diagram for the MAFC setup.

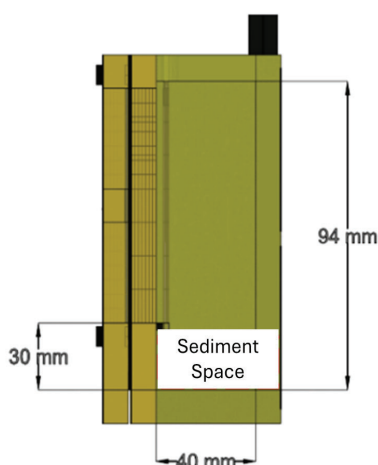


FIGURE 2. Modified watery single cell Mg–air cell

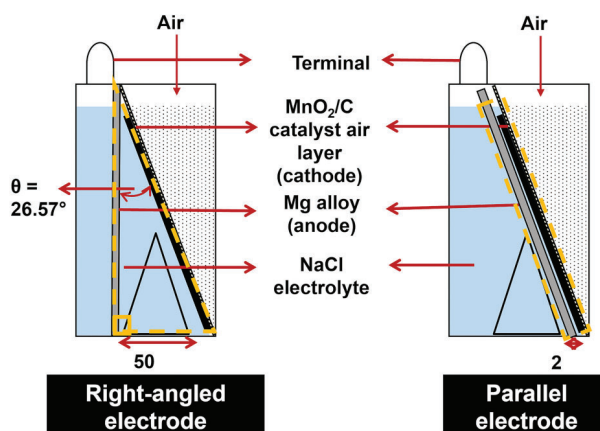


FIGURE 3. Schematic diagram of Mg–air cell configuration with Mg anode is 26.57° away from air cathode (left) and with Mg anode is parallel with air cathode (right)

ELECTROLYTE VOLUME (V)

Three different volumes of electrolyte are varied to investigate the effect of electrolyte volume on the performance of MAFC. This is crucial to determine the suitable and optimum size of the cell which may influence the practical application of MAFC. The manipulated volume of electrolyte for performance test with varying size of chamber and volume which are 0.5 L (V1), 1 L (V2), and 1.6 L (V3) using 3.5 wt.% NaCl solution and right-angled electrode position.

ELECTRODE POSITION (P)

Due to the overall reaction in the electrolyte producing precipitation product that will deposit at the surface of electrodes and subsequently blocking and reducing the active area of electrodes, it is essential to investigate if putting a distance between electrodes in certain way can make a difference on cell performance. In this work, the electrodes were positioned in two ways, i.e., right-angled with a 50 mm gap at the bottom between the electrodes (P1) and parallel to each other with 2 mm gap between them (P2), as shown in Figure 3, to find the effect of distance between electrodes on cell performance. The electrolyte used in this experiment was 3.5 wt.% NaCl in 0.5 L container.

ELECTROLYTE CONCENTRATION (C)

Concentration of electrolyte certainly affects the performance of MAFC. Hence, three different concentrations of NaCl solution which are 3.5 wt.% (C1), 5 wt.% (C2), and 10 wt.% (C3) were tested to find the best electrolyte concentration to obtain the highest cell performance.

CORROSION EVALUATION

Hydrogen evolution tests of AZ31 were conducted at room temperature, and the solutions were prepared using analytical-grade sodium chloride (NaCl) salt to determine the corrosion rate of magnesium anode in different NaCl concentrations and in the presence of sodium phosphate (Na_3PO_4) as additive in electrolyte. Magnesium alloy plate was cut into small blocks to the size of 10 mm × 10 mm × 1 mm. The surface of the sample was grounded with silicon carbide sandpaper up to 1500 grit to remove the oxidized layer and provide a smoother surface. After polished, the samples were cleaned with alcohol, air-dried, and weighed. After

weighed, the samples were sealed with epoxy resin, leaving an exposed area of 10 mm × 10 mm to be immersed into electrolyte mentioned earlier for 48 hours using a typical setup for corrosion testing (Feyerabend 2014). The average corrosion rate was estimated according to the average evolution rate for hydrogen using the Eq. (1):

$$v_{\text{H}_2} = \frac{V_{\text{H}_2}}{st} \quad (1)$$

where H_2 represents the average rate of hydrogen evolution ($\text{mL cm}^{-2}\text{h}^{-1}$), V_{H_2} is the total volume of hydrogen evolution (mL), s is the sample surface (cm^2), and t is the immersion time (h) (Zheng et al. 2018).

Meanwhile, the inhibition efficiency was calculated using the Eq. (2):

$$\text{IE} = \frac{v - v_0}{v} \times 100\% \quad (2)$$

where v is corrosion rate without additive and v_0 is corrosion rate with additive (Li et al. 2018).

The surface morphology of samples was analysed using scanning electron microscope (SEM: CARL ZEISS EVO MA10) equipped with energy dispersive X-ray (EDX) before and after the immersion test in NaCl 3.5 wt.% and NaCl 3.5 wt.% with additive for comparison. Samples before immersion test were etched with 5% Nital solution to reveal the microstructure.

RESULTS AND DISCUSSION

ELECTROLYTE VOLUME (V)

The effect of electrolyte volume on MAFC performance was tested in 3.5 wt.% NaCl solution with right-angled positioned electrode. Based on Figure 4, MAFC performance shows little difference in various volumes where MAFC with 0.5 L, 1 L, and 1.6 L of electrolyte volume yields 9.22 mW cm^{-2} , 10.8 mW cm^{-2} , and 8.86 mW cm^{-2} respectively. It is a basic understanding that only ions travel in solution in an electrochemical cell whereas the electrons travel through the wire between the electrodes and never enter the solution. The electrons moving through the wires and the ions moving freely in the solution maintain the flow of electricity in the circuit. Apart from that, the amount or concentration of ion depends on the concentration of solution as in the higher the concentration

of solution, the higher the concentration of ion would be (Ben-Hamu et al. 2010). Hence, regardless of the amount of electrolyte, the same concentration of solution would have same concentration of ion with same electron flow behavior where the cation will move towards the cathode and the anions will move towards the anode. This also means that volume of electrolyte does not play a significant role in the changes of current nor the voltage in MAFC performance. This is advantageous to have smaller and compact design of MAFC for portable application. However, smaller volume of electrolyte could increase ohmic resistance and charge transfer resistance in a lithium-ion battery system (An et al. 2017a).

The peak performance was observed at 1 L of electrolyte, indicating a potential optimal volume for maximizing power output. However, the differences in performance across the volumes (9.22 mW cm⁻² to 10.8 mW cm⁻²) are not substantial, suggesting that the MAFC is relatively robust to changes in electrolyte volume within the 0.5 L to 1.6 L range. This indicates that while electrolyte volume does influence the performance of MAFCs, the effect is not markedly significant, implying that other factors, such as electrode configuration, reaction activity, or ion concentration, may play more critical roles in determining the overall efficiency and performance of the system.

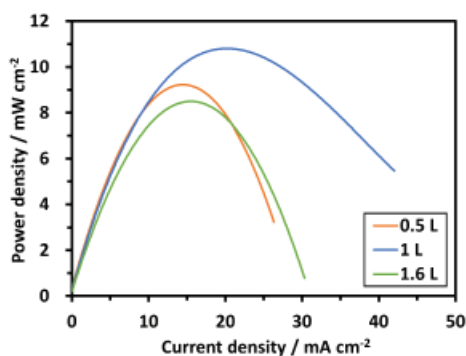


FIGURE 4. Performance of MAFC with different electrolyte volume

ELECTRODE POSITION (P)

Since volume is not a critical factor in MAFC performance, 0.5 L volume of electrolyte is applied in the cell setup for the next experiment which is to investigate the effect of electrode positioning in MAFC. Figure 5 depicted the performance of MAFC with different electrode positions in MAFC configuration. It is obvious that MAFC with parallel-positioned electrodes yields higher performance (17.42 mW cm⁻²) than MAFC with right-angled electrode positioned (9.22 mW cm⁻²). This shows that the distance between electrodes plays an important role in configuration of MAFC to obtain optimum cell performance. The further the distance between the electrode, the longer the time it takes for the ion to travel from one electrode to another, the more the internal resistance, which lowers the performance of the cell (Sajana et al. 2013). Nagai et al. also found that increasing the space between a pair of electrodes increases the electrical resistance between the electrodes that, thereby decreasing the electrical current in

water electrolysis (Nagai et al. 2003). However, electrodes that are very close to each other increase the void fraction or production of bubbles between the electrodes, thus increasing electrical resistance and leading to inefficiency of water electrolysis process (LeRoy et al. 1979; Mazloomi & Sulaiman 2012). Thor et al. added that the resistance flow of ions is reduced when the electrode distance is closer, thus improving the mass transfer of ion between electrodes (Thor et al. 2022). Similar results were also observed for microbial fuel cells where smaller gap between the electrodes could enhanced the cell performance (Moon et al. 2015). Considering that all the reactions of Mg-air fuel cell occur in the electrolyte, the effect of void fraction on Mg-air cell performance should be studied to have better understanding from cell configuration perspective. Herein, it is decided that the MAFC system with parallel electrode position and 0.5 L electrolyte volume was the optimum system configuration to be used in the following study to elucidate the effect of electrolyte concentration on MAFC performance.

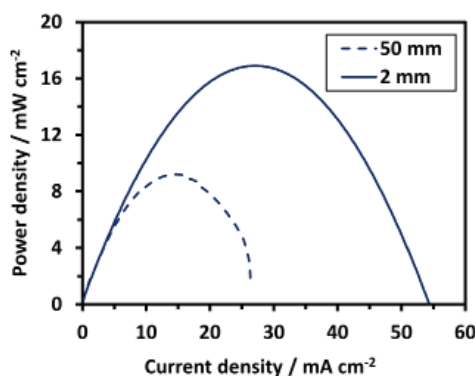


FIGURE 5. Performance of MAFC with different distance between electrodes

ELECTROLYTE CONCENTRATION (C)

MAFC with parallel-positioned electrodes and 0.5 L electrolyte volume was used as the final configuration to test the effect of NaCl concentration as electrolyte. Based on Figure 6, MAFC with 10 wt% NaCl solution as electrolyte yielded the highest power density (38.95 mW cm^{-2}), followed by the cell using 5 wt.% NaCl solution (23.9 mW cm^{-2}), and cell with 3.5% NaCl solution yielded the lowest power density (17.42 mW cm^{-2}). This result supports the findings of a previous study, in which the higher the concentration of NaCl, the higher the power density yield because of the increase of chloride ion in the solution (Acharya & Shetty 2019). The Arrhenius theory, which says that an electrolyte solution's ionic conductivity is determined by its electrolyte ions, can be used to explain this finding. A medium's capacity to conduct electricity is demonstrated by its conductivity. As a result, a solution with high concentrations of sodium and chloride ions that reduces the resistivity for ion propagation will have high conductivity making electricity can conveniently flow

through it thus may increasing the power produced by the cell (Widodo et al. 2018) [48]. It is worthy to note that the fluctuation highlighted in the red box in the graph is due to phenomena of precipitation product attached and detached from the electrodes surface. As the concentration of NaCl decreases, the ionic strength decreases as well, which can have an effect on the conductivity of the electrolyte. It is possible that this will result in lower current outputs because the movement of ions is essential for the transfer of charge within the cell. Although magnesium hydroxide is easily attached on the anode surface, the precipitation layer is thin and porous, making it easily detached from the anode surface because of its low solubility property related to its low Gibbs free energy, ($-833.7 \text{ kJ mol}^{-1}$) which builds a high energy barrier and makes it harder to dissolve in aqueous solution (Weber et al. 2021). Hence, when the precipitation product forms a thin protective layer covering the anode surface, the performance begins to drop. When the layer becomes unstable due to corrosive Cl^- attack, it falls off the anode surface, exposing the reactive area for reaction and increasing performance (Merino et al. 2010).

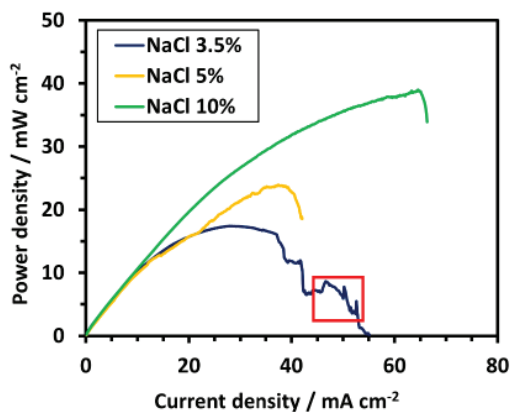


FIGURE 6. Performance of MAFC using different NaCl solutions. Red box indicate the phenomena of precipitation product attached and detached from the electrodes surface.

CORROSION EVALUATION

Despite increasing the cell performance, increasing NaCl concentration also increases the rate of corrosion for Mg anode. Based on Figure 7, 10% NaCl solution had the highest corrosion rate, followed by 5% NaCl solution, and then 3.5% NaCl solution. This finding is in line with previous study where the higher the concentration of NaCl, the more the Cl⁻ ion, the higher the corrosion rate (Basri et al. 2020; Dhanapal et al. 2012; Hazri et al. 2021). Mg has a natural affinity to oxidise quickly in any environment that contains oxygen or water. This is because Mg has a very low standard electrode potential (2.37 V vs. SHE), which makes it very easy for it to lose an electron and form an ion and get oxidised. The vigorous Mg interaction with electrolytes is what causes the Mg anode to corrode severely, meanwhile the oxygen reduction reaction kinetics

from the air cathode behave in the opposite way when exposed to aqueous solution. The corrosion reactions in the solution can be explained with Eqs. (3)-(6):

$$IE = \frac{v - v_0}{v} \times 100\% \quad (2)$$

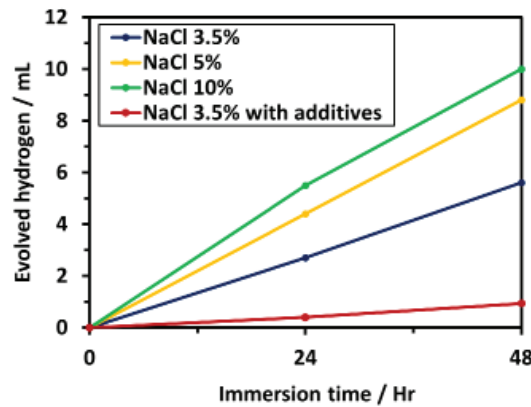
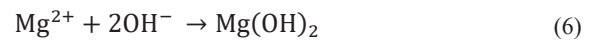
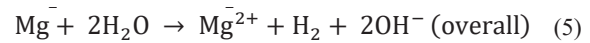


FIGURE 7. Hydrogen evolution test

Firstly, the anodic reaction at the anode site will generate Mg ion and electron (Eq.3). Simultaneously, the catalyst at the cathode site will catalyze the oxygen reaction to produce hydrogen ion and hydroxide ion (Eq.4). So, the overall reaction occurring in the solution as soon as Mg anode is immersed in the solution will produce Mg ion, hydroxide ion, and hydrogen gas (Eq.5). The Mg ion and hydroxide ion will react together to form magnesium hydroxide (Eq.6) which will accumulate and precipitate on the surface of Mg anode over time becoming a protective layer. However, the Mg (OH)₂ layer is a weak layer and easily detached from anode surface because it can easily dissolve in the solution again. So when chloride ion is increased, the weak precipitation layer is susceptible the aggressive nature of chloride ion causing it breakdown and exposing the anode surface to the solution which further initiates localized corrosion (Shi et al. 2017) [54, 55]. Magnesium forms a protective oxide/hydroxide layer

(Mg(OH)₂) that slows down the corrosion process. However, Cl⁻ ions are highly aggressive and can penetrate this passive layer, causing localized breakdown and pitting corrosion as shown in chemical equation 7.



The interaction between Mg(OH)₂ and chloride ions (Cl⁻) is crucial in the corrosion mechanism of magnesium in saline environments. When chloride ions (Cl⁻) mix with the naturally occurring layer of Mg(OH)₂ on the surface of magnesium, a chemical reaction takes place, leading to the creation of magnesium chloride (MgCl₂), which is a highly soluble compound in water. The presence of soluble MgCl₂ causes the dissolution and elimination of the protective Mg(OH)₂ layer, hence removing the barrier that protects the underlying magnesium from direct contact with the corrosive surroundings.

The solubilization step is crucial as it prevents the magnesium metal from undergoing further oxidation by forming a protective covering of $\text{Mg}(\text{OH})_2$. The transformation into MgCl_2 compromises the integrity of the protective barrier as it can be easily washed away by the surrounding electrolyte solution. As a result, the magnesium metal beneath is uncovered and becomes exposed to the surrounding NaCl solution. After the removal of the protective $\text{Mg}(\text{OH})_2$ layer, the freshly exposed magnesium surface becomes extremely susceptible to further electrochemical processes. These processes usually entail the anodic dissolution of magnesium, in which magnesium atoms relinquish electrons to create magnesium ions (Mg^{2+}). Concurrently, cathodic reactions, such as the process of reducing oxygen in the presence of water, generate hydroxide ions (OH^-).

The continuous interaction between newly exposed magnesium and chloride ions sustains a cycle of corrosion. During the formation of $\text{Mg}(\text{OH})_2$ from the reaction between Mg^{2+} and OH^- ions, it is once again subjected to attack by Cl^- ions. This results in the production of more MgCl_2 and the dissolution of the newly formed protective layer. The recurring pattern causes continuous deterioration of the magnesium metal, as each subsequent layer of $\text{Mg}(\text{OH})_2$ is progressively eliminated, revealing new magnesium that is continuously subjected to corrosive damage. After adding 0.1 wt.% of sodium phosphate in 3.5 wt.% NaCl solution, the corrosion rate of Mg anode is significantly reduced, and cell performance was also improved by 66% (22.32 mW cm^{-2}) as shown in Figure 8.

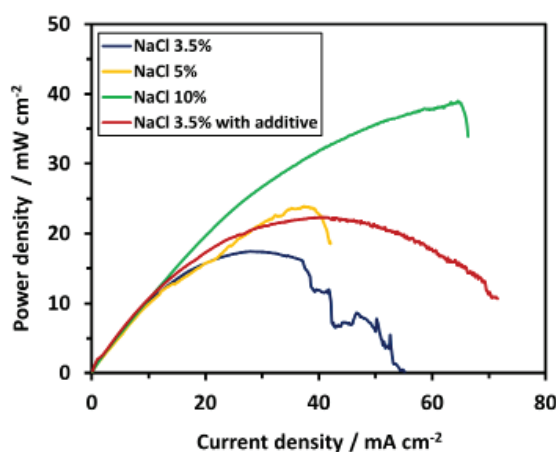


FIGURE 8: Performance of MAFC using 0.5L of NaCl 3.5% NaCl electrolyte with and without additive

This is because magnesium ion reacts with phosphate ion to form $\text{Mg}_3(\text{PO}_4)_2$ layer (Eq.7). This layer is more compact and denser than $\text{Mg}(\text{OH})_2$ layer owing to the smaller solubility-product K_{sp} value (1.04×10^{-24}), which means that $\text{Mg}_3(\text{PO}_4)_2$ layer is less likely to dissolve back into the solution unlike $\text{Mg}(\text{OH})_2$ layer, hence $\text{Mg}_3(\text{PO}_4)_2$ able to provide a better protective layer for Mg anode against chloride ions attack (Hou et al. 2016; Li et al. 2018). This result is further confirmed by SEM observation of the surface microstructure before immersion test (a and b), after immersion in NaCl 3.5 wt.% without additive (c and d), and immersion in NaCl 3.5 wt.% with additive in Figure 9. Sample immersed in NaCl 3.5 wt.% has large lumpy precipitation product (Figure 9d) compared to the sample immersed in solution containing additive which has small flaky dandruff-like product (Figure 9f). The crack feature (red arrow) caused by aggressive attack of the chloride ion

as explained above were more obvious on the samples in solution without additive than samples in solution with additive. The EDX analysis (Figure 10b) also clearly shows that the oxygen element has reduced greatly in sample immersed in solution containing additive compared to its counterparts (Figure 10a). Using 0.1 wt% of sodium phosphate shows 83.3% inhibition efficiency which is higher than using 0.005 wt% of sodium phosphate used for AZ91 in previous work (Li, Yaqiong, Jingling Ma, Guangxin Wang, Fengzhang Ren, Yujie Zhu et al. 2018). This prove that adding sodium phosphate as additive could prevent the formation of typical precipitation product, magnesium hydroxide, and improve the corrosion resistance for MAFC as shown in chemical equation 8.



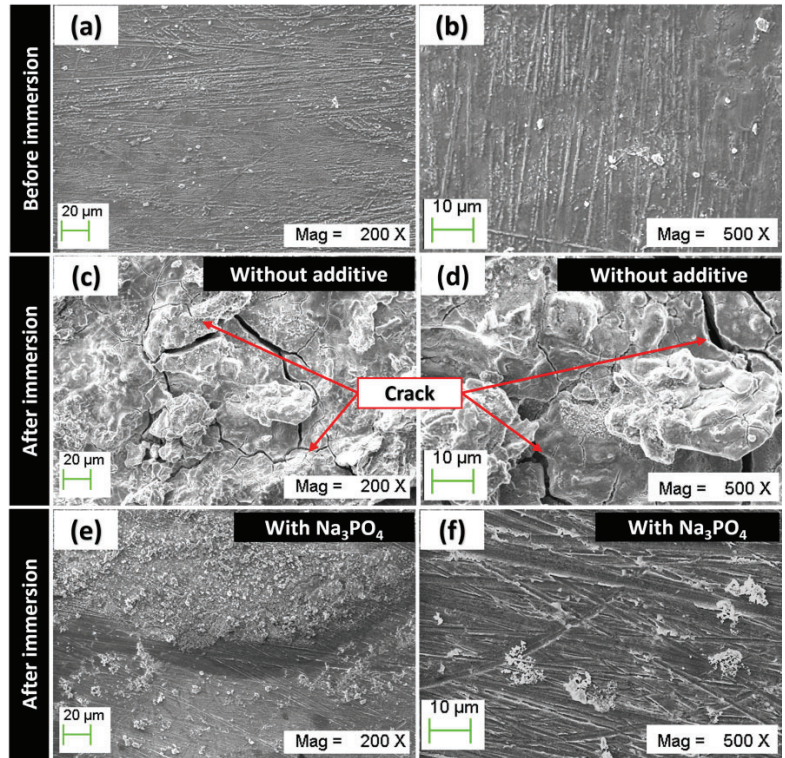


FIGURE 9: Surface morphology of AZ31 before immersion (a and b), after immersion in NaCl 3.5% (c and d) without additive and (e and f) with additive

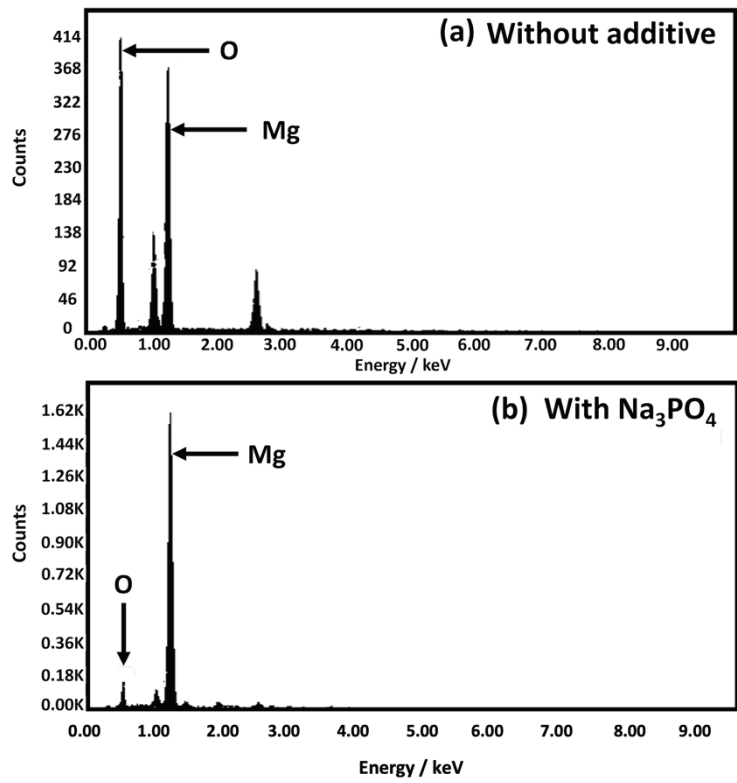


FIGURE 10. EDX analysis of AZ31 in NaCl 3.5% a) without additive and b) with additive

Table 1 summarized the performance for all experiment while Table 2 shows comparison of inhibition

efficiency with other additives used for MAFC in previous work.

TABLE 1. Summary of studied MAFC performance

Electrolyte volume / L	Electrode position	NaCl concentration / wt.%	Additive	Power density / mW cm ⁻²	OCV / V
1.6			-	8.86	1.66
1.0	Right angle	3.5	-	10.8	1.47
0.5			-	9.22	1.77
		3.5	-	17.42	1.68
	Parallel	5	-	23.9	1.5
0.5		10	-	38.95	1.67
		3.5	0.1 wt.% Na ₃ PO ₄	22.32	2.46

TABLE 2. Comparison of inhibition efficiency with other additives used for MAFC

Anode	Electrolyte	Additive	Inhibition efficiency / %	Ref.
AZ91	3.5% NaCl	0.05 g L ⁻¹ sodium phosphate	65.1	(Li et al. 2018)
		0.01 M sodium citrate	85	
AM60	0.1 M NaCl	0.01 M SDBS	93	(Liu et al. 2018)
		0.01 M diammonium phosphate	79	
		0.01 M sodium vanadate	77	
AZ31	0.1 M NaCl	50 mM sodium carbonate	76	(Prince et al. 2021)
AZ31	3.5% NaCl	0.1 wt% sodium phosphate	83	This work

APPLICATION OF SALTS TYPE

Seawater, table salt, and analytical grade NaCl contain different sodium chloride ion concentration and purity. Commercial table salt may undergo different manufacturing processes such as mining for rock salt, water evaporation for lake and sea salt, and wells for river and well salts in non-coastal state (Renzi et al. 2019). Table salts commonly consist of 97% to 99% of sodium chloride and very small amount of other compound such as potassium chloride and magnesium chloride depending on the source and manufacturer while analytical grade NaCl usually made up of rock salt with high purity containing only sodium chloride. Meanwhile, chemical composition of seawater is made up of many different dissolved salts from various elements found naturally. There are six major ions in seawater which are chloride (Cl⁻), sodium (Na⁺), sulfate (SO₄²⁻), magnesium (Mg²⁺), calcium (Ca²⁺), and potassium (K⁺). These ions made up almost 99% of the seawater by weight. Hence, it is intriguing to investigate and compare

the performance of MAFC using natural seawater, commercial table salts, and pure NaCl as electrolytes.

Performance tests were performed using natural seawater taken from estuary of Sepang River, commercial iodate fine table salts, and pure NaCl analytical grade supplied by Sigma Aldrich as electrolyte. Both table salts and pure NaCl were dissolved in deionized water to produce a salt solution with a concentration of 3.5 wt.% to be consistent with seawater salinity. Figure 11 depicted the performance of MAFC using natural seawater, table salts, and pure NaCl. From the figure, it shows that MAFC using pure NaCl as electrolyte has the highest performance (28.12 mW cm⁻²), followed by seawater (20.43 mW cm⁻²), and the lowest performance is cell using table salt is electrolyte (17.42 mW cm⁻²). Even though all three solutions have similar concentration of sodium chloride (3.5 wt.%), it yields different performance probably owing to its different purity level and contaminants or impurities that affects the overall performance as different compound could behave differently with the magnesium anode. It can

be said that high purity level which contain only sodium chloride is the best quality of salt to harness the best performance from MAFC cell. Seawater electrolyte shows slightly better performance probably due to having abundance of different kinds of anion that made the

electrolyte more conductive than table salt electrolyte. However, to make MAFC more feasible for commercialization in domestic areas, the consumer can simply increase the amount of table salts used to increase the power of MAFC to provide the energy needed.

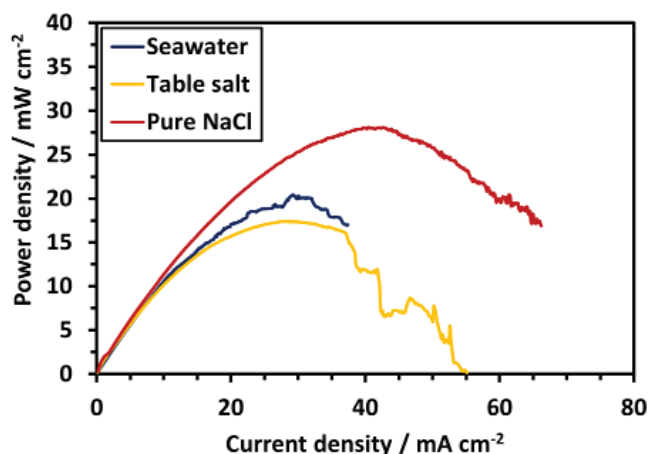


FIGURE 11. Performance comparison using different kind of salts

CONCLUSIONS

The main objective in this study is to find the best cell configuration for MAFC to produce optimum performance by investigating the effect of electrolyte volume, electrodes position, and electrolyte concentration on performance of Mg–air fuel cell. Though from the investigation shows that volume of electrolyte is not crucial factor in MAFC performance unlike position of electrode, volume of electrode and configuration. Although the corrosion rate is highest in 10% NaCl solution, the high concentration of chloride ion in the solution along with the short distance that the ion needs to travel from one electrode to another manage to increase the power density of MAFC proving that electrode position plays a vital role in cell configuration of MAFC. Based on the result obtained, MAFC with parallel position of electrode, smallest electrolyte volume (0.5 L), and highest electrolyte concentration (10 wt.% NaCl solution) yielded the best performance with power density of 38.95 mW cm⁻². The severe corrosion issue could be overcome by adding corrosion inhibitor such as sodium phosphate that can form a better protective layer replacing the weak and porous Mg (OH)₂ layer which could hinder further corrosion reaction on Mg anode surface. This work clearly shows that cell configuration involving electrode position and electrolyte volume do play important role affecting the performance of MAFC and worthy to pay attention to for further research. This study is very important to obtain early stage data before scaling up to

produce higher power. This MAFC has great potential to produce power up to 100 W for the use of portable equipment such as car batteries.

ACKNOWLEDGEMENTS

The author would like to acknowledge the Minister of Higher Education under the Fundamental Research Grant Scheme (FRGS) FRGS/1/2020/STG04/UKM/03/1 and HiCoE (SELFUEL): HiCoE-2023-001.

DECLARATION OF COMPETING INTEREST

None.

REFERENCES

- Acharya, M.G. & Shetty, A.N. 2019. The corrosion behavior of AZ31 alloy in chloride and sulfate media – A comparative study through electrochemical investigations. *Journal of Magnesium and Alloys* 7(1): 98–112.
- Alloys, J.W.-J. of M. and & 2021, undefi ned. (n.d.). Exploring the concept of castability in magnesium die-casting alloys. *Elsevier*.

- Amjad Javaid & Frank Czerwinski. 2021. Progress in twin roll casting of magnesium alloys: A review. *Journal of Magnesium and Alloys* 9(2): 362–391.
- An, S.J., Li, J., Daniel, C., Meyer, H.M., Trask, S.E., Polzin, B.J. & Wood, D.L. 2017a. Electrolyte volume effects on electrochemical performance and solid electrolyte interphase in si-graphite/NMC lithium-ion pouch cells. *ACS Applied Materials and Interfaces* 9(22): 18799–18808.
- An, S.J., Li, J., Mohanty, D., Daniel, C., Polzin, B.J., Croy, J.R., E. Trask, S. & Wood, D.L. 2017b. Correlation of electrolyte volume and electrochemical performance in lithium-ion pouch cells with graphite anodes and NMC532 cathodes. *Journal of The Electrochemical Society* 164(6): A1195–A1202.
- Ashassi-Sorkhabi, H., Moradi-Alavian, S. & Kazempour, A. 2019. Salt-nanoparticle systems incorporated into sol-gel coatings for corrosion protection of AZ91 magnesium alloy. *Progress in Organic Coatings* 135: 475–482.
- Basri, S., Hazri, N.S., Selladurai, S.R., Zainoodin, A.M., Kamarudin, S.K., Zakaria, S.U. & Hashim, A.R. 2020. Analysis of Mg(OH)₂ deposition for Magnesium Air Fuel Cell (MAFC) by saline water. *Sains Malaysiana* 49(12): 3105–3115.
- Ben-Hamu, G., Eliezer, D. & Shin, K.S. 2010. Studies on the influence of chloride ion concentration on the corrosion behavior of zsmx magnesium alloy. *Advanced Materials Research* 95: 47–50.
- Chen, X., Ning, S., Le, Q., Wang, H., Zou, Q., Guo, R., Hou, J., Jia, Y., Atrens, A. & Yu, F. 2020. Effects of external field treatment on the electrochemical behaviors and discharge performance of AZ80 anodes for Mg-air batteries. *Journal of Materials Science and Technology* 38: 47–55.
- Chen, X., Zou, Q., Le, Q., Zhang, M., Liu, M. & Atrens, A. 2022. Influence of heat treatment on the discharge performance of Mg-Al and Mg-Zn alloys as anodes for the Mg-air battery. *Chemical Engineering Journal* 433.
- Deng, M., Höche, D., Lamaka, S. V., Wang, L. & Zheludkevich, M.L. 2019. Revealing the impact of second phase morphology on discharge properties of binary Mg-Ca anodes for primary Mg-air batteries. *Corrosion Science* 153: 225–235.
- DENG, M., WANG, R. chu, FENG, Y., WANG, N. guang & WANG, L. qian. 2016. Corrosion and discharge performance of Mg–9%Al–2.5%Pb alloy as anode for seawater activated battery. *Transactions of Nonferrous Metals Society of China (English Edition)* 26(8): 2144–2151.
- Dhanapal, A., Rajendra Boopathy, S. & Balasubramanian, V. 2012. Influence of pH value, chloride ion concentration and immersion time on corrosion rate of friction stir welded AZ61A magnesium alloy weldments. *Journal of Alloys and Compounds Complete*(523): 49–60.
- Dong, X., Wang, J., Wang, X., Yang, J., Zhu, L., Zeng, W., Huang, G., Wang, J. & Pan, F. 2022. Prussian blue analogue derived Co₃O₄/CuO nanoparticles as effective oxygen reduction reaction catalyst for magnesium-air battery. *Journal of The Electrochemical Society* 169(1): 010532.
- Feyerabend, F. 2014. In vitro analysis of magnesium corrosion in orthopaedic biomaterials. *Biomaterials for Bone Regeneration: Novel Techniques and Applications*: 225–269.
- Gielen, D., Boshell, F., Saygin, D., Bazilian, M.D., Wagner, N. & Gorini, R. 2019. The role of renewable energy in the global energy transformation. *Energy Strategy Reviews* 24: 38–50.
- Guo, X., Hu, Y., Yuan, K. & Qiao, Y. 2022. Review of the effect of surface coating modification on magnesium alloy biocompatibility. *Materials (Basel, Switzerland)* 15(9).
- Häcker, J., Rommel, T., Lange, P., Zhao-Karger, Z., Morawietz, T., Biswas, I., Wagner, N., Nojabaei, M. & Friedrich, K.A. 2023. Magnesium anode protection by an organic artificial solid electrolyte interphase for magnesium-sulfur batteries. *ACS Applied Materials & Interfaces* 15(27): 33013–33027.
- Hazri, N.S., Basri, S., Kamarudin, S.K. & Zainoodin, A.M. 2021. Critical review on development of magnesium alloy as anode in Mg-Air fuel cell and additives in electrolyte. *International Journal of Energy Research* 45(11): 15739–15759.
- Hou, L., Dang, N., Yang, H., Liu, B., Li, Y., Wei, Y. & Chen, X.-B. 2016. A combined inhibiting effect of sodium alginate and sodium phosphate on the corrosion of magnesium alloy AZ31 in NaCl solution. *Journal of The Electrochemical Society* 163(8): C486–C494.
- Kim, D.H., Jang, K.H., Jang, K., Shin, K.S., Kim, H.S., Kim, S.O., Kim, K.B. & Chung, K.Y. 2022. Effect of optimum current-collector design on electrochemical performance of Mg-air primary batteries for large-scale energy storage. *International Journal of Energy Research* 46(11): 15837–15849.
- Lamaka, S. V., Vaghefinazari, B., Mei, D., Petrauskas, R.P., Höche, D. & Zheludkevich, M.L. 2017. Comprehensive screening of Mg corrosion inhibitors. *Corrosion Science* 128: 224–240.
- LeRoy, R.L., Janjua, M.B.I., Renaud, R. & Leuenberger, U. 1979. Analysis of time-variation effects in water electrolyzers. *Journal of The Electrochemical Society* 126(10): 1674–1682.
- Li, Y., Ma, J., Wang, G., Ren, F., Zhu, Y. & Song, Y. 2018. Investigation of sodium phosphate and sodium dodecylbenzenesulfonate as electrolyte additives for AZ91 magnesium-air battery. *Journal of The Electrochemical Society* 165(9): A1713–A1717.
- Li, Yaqiong, Jingling Ma, Guangxin Wang, Fengzhang Ren, Yujie Zhu, and Y.S., Li, Y., Ma, J., Wang, G., Ren, F., Zhu, Y., Song, Y. & Li Yaqiong, Jingling Ma, Guangxin Wang, Fengzhang Ren, Yujie Zhu,

- and Y.S. 2018. Investigation of sodium phosphate and sodium dodecylbenzenesulfonate as electrolyte additives for AZ91 magnesium-air battery. *Journal of the Electrochemical Society* 165(9): A1713–17.
- Liu, D., Song, Y., Shan, D. & Han, E.H. 2018. Comparison of the inhibition effect of four inhibitors on the corrosion behaviour of AM60 magnesium alloy. *International Journal of Electrochemical Science* 13(3): 2219–2235.
- Liu, Q., Pan, Z., Wang, E., An, L. & Sun, G. 2020. Aqueous metal-air batteries: Fundamentals and applications. *Energy Storage Materials* 27: 478–505.
- Luo, Y., Deng, Y., Guan, L., Ye, L. & Guo, X. 2020. The microstructure and corrosion resistance of as-extruded Mg-6Gd-2Y- (0–1.5) Nd-0.2Zr alloys. *Materials and Design* 186.
- Mazloomi, S.K. & Sulaiman, N. 2012. Influencing factors of water electrolysis electrical efficiency. *Renewable and Sustainable Energy Reviews* 16(6): 4257–4263.
- Merino, M.C., Pardo, A., Arrabal, R., Merino, S., Casajús, P. & Mohedano, M. 2010. Influence of chloride ion concentration and temperature on the corrosion of Mg–Al alloys in salt fog. *Corrosion Science* 52(5): 1696–1704.
- Moon, J.M., Kondaveeti, S., Lee, T.H., Song, Y.C. & Min, B. 2015. Minimum interspatial electrode spacing to optimize air-cathode microbial fuel cell operation with a membrane electrode assembly. *Bioelectrochemistry (Amsterdam, Netherlands)* 106(Pt B): 263–267.
- Nagai, N., Takeuchi, M., Kimura, T. & Oka, T. 2003. Existence of optimum space between electrodes on hydrogen production by water electrolysis. *International Journal of Hydrogen Energy* 28(1): 35–41.
- Prince, L., Rousseau, M.A., Noifalisse, X., Dangreau, L., Coelho, L.B. & Olivier, M.G. 2021. Inhibitive effect of sodium carbonate on corrosion of AZ31 magnesium alloy in NaCl solution. *Corrosion Science* 179: 109131.
- Renzi, M., Grazioli, E., Bertacchini, E. & Blašković, A. 2019. Microparticles in table salt: Levels and chemical composition of the smallest dimensional fraction. *Journal of Marine Science and Engineering* 2019, Vol. 7, Page 310 7(9): 310.
- Sajana, T.K., Ghangrekar, M.M. & Mitra, A. 2013. Effect of pH and distance between electrodes on the performance of a sediment microbial fuel cell. *Water science and technology: a journal of the International Association on Water Pollution Research* 68(3): 537–543.
- Saji, V.S. 2023. Corrosion and materials degradation in electrochemical energy storage and conversion devices. *ChemElectroChem* 10(11).
- Samarasingha, P.B., Lee, M.-T. & Valvo, M. 2021. Reactive surface coating of metallic lithium and its role in rechargeable lithium metal batteries. *Electrochimica Acta* 397: 139270.
- Shi, Y., Peng, C., Feng, Y., Wang, R. & Wang, N. 2017. Enhancement of discharge properties of an extruded Mg–Al–Pb anode for seawater-activated battery by lanthanum addition. *Journal of Alloys and Compounds* 721: 392–404.
- Simeon, M.I. & Freitag, R. 2022. Influence of electrode spacing and fed-batch operation on the maximum performance trend of a soil microbial fuel cell. *International Journal of Hydrogen Energy* 47(24): 12304–12316.
- Song, G. & Atrens, A. 2003. Understanding magnesium corrosion. A framework for improved alloy performance. *Advanced Engineering Materials* 5(12): 837–858.
- Song, G.L. 2013a. Corrosion behavior and prevention strategies for magnesium (Mg) alloys. *Corrosion Prevention of Magnesium Alloys: A volume in Woodhead Publishing Series in Metals and Surface Engineering*: 3–37.
- Song, G.L. 2013b. Corrosion behavior and prevention strategies for magnesium (Mg) alloys. *Corrosion Prevention of Magnesium Alloys: A volume in Woodhead Publishing Series in Metals and Surface Engineering*: 3–37.
- Thor, S.H., Ho, L.N., Ong, S.A., Abidin, C.Z.A., Heah, C.Y., Nordin, N., Ong, Y.P. & Yap, K.L. 2022. Discovering the roles of electrode distance and configuration in dye degradation and electricity generation in photocatalytic fuel cell integrated electro-Fenton process. *Separation and Purification Technology* 278.
- Tong, F., Wei, S., Chen, X. & Gao, W. 2021. Magnesium alloys as anodes for neutral aqueous magnesium-air batteries. *Journal of Magnesium and Alloys* 9(6): 1861–1883.
- Weber, I., Ingenmey, J., Schnaidt, J., Kirchner, B. & Behm, R.J. 2021. Influence of complexing additives on the reversible deposition/dissolution of magnesium in an ionic liquid. *ChemElectroChem* 8(2): 390–402.
- Widodo, C.S., Sela, H. & Santosa, D.R. 2018. The effect of NaCl concentration on the ionic NaCl solutions electrical impedance value using electrochemical impedance spectroscopy methods. *AIP Conference Proceedings* 2021(1): 50003.
- Xue, Y., Miao, H., Sun, S., Wang, Q., Li, S. & Liu, Z. 2015. Template-directed fabrication of porous gas diffusion layer for magnesium air batteries. *Journal of Power Sources* 297: 202–207.
- Zai, W., Zhang, X., Su, Y., Man, H.C., Li, G. & Lian, J. 2020. Comparison of corrosion resistance and biocompatibility of magnesium phosphate (MgP), zinc phosphate (ZnP) and calcium phosphate (CaP) conversion coatings on Mg alloy. *Surface and Coatings Technology* 397.

- Zhang, T., Tao, Z. & Chen, J. 2014. Magnesium–air batteries: from principle to application. *Materials Horizons* 1(2): 196–206.
- Zhang, X. man, Chen, Z. yu, Luo, H. feng, Zhou, T., Zhao, Y. liang & Ling, Z. cheng. 2022. Corrosion resistances of metallic materials in environments containing chloride ions: A review. *Transactions of Nonferrous Metals Society of China (English Edition)* 32(2): 377–410.
- Zhao, T., Niu, S., Wu, X., Wu, Q., Ma, Z., Jiang, J., Huang, Y., Wang, H., Li, Q. & Cai, Y. 2022a. Manganese decoration tailored nitrogen doping for boosted oxygen reduction electrocatalysis of Co-NC. *Journal of Alloys and Compounds* 924: 166532.
- Zhao, T., Wei, S., Niu, S., Wu, Q., Liu, K., Ma, Z., Huang, Y., Wang, H., Cai, Y. & Li, Q. 2022b. Thermal migration promotes the formation of manganese and nitrogen doped polyhedral surface for boosted oxygen reduction electrocatalysis. *Inorganic Chemistry* 61(33): 13165–13173.
- Zheng, T., Hu, Y., Zhang, Y., Yang, S. & Pan, F. 2018. Composition optimization and electrochemical properties of Mg-Al-Sn-Mn alloy anode for Mg-air batteries. *Materials & Design* 137: 245–255.
- Zhou, J., He, X., Zhou, Z. & Li, F. 2022. Cu ion doping α -MnO₂ nanowire electrocatalysts for Mg-air battery. *Journal of Solid State Electrochemistry* 26(2): 335–341.